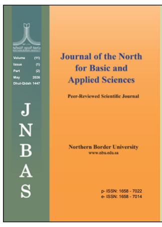

KINGDOM OF SAUDI ARABIA
Northern Border University (NBU)
Journal of the North for Basic & Applied Sciences(JNBAS)
p - ISSN : 1658 -7022 / **e-ISSN:** 1658 - 7014
www.nbu.edu.sa
s.journal@nbu.edu.sa

Analytical Solutions of Fractional Stochastic Wazwaz-Benjamin-Bona-Mahony Equations

Ahmed M. A. Adam
Department of Mathematics, College of Science, Northern Border University, Arar, Saudi Arabia

(**Received:** 6th December 2025; **Accepted:** 25th Jan 2026)

Abstract
This study examines a group of fractional stochastic Wazwaz-Benjamin-Bona-Mahony (FSWBBM) Equations, which incorporate both fractional and stochastic perturbations. The Wazwaz-Benjamin-Bona-Mahony (WBBM) Equations are widely adopted to describe the nonlinear behaviors of waves in dispersive media. The main objective in this study is to develop exact travelling wave solutions through an advanced analytical technique. In this framework, the Riccati-Bernoulli sub-ODE (R-B S-ODE) method is applied, replacing the classical derivatives with a conformable fractional derivative of order $\vartheta \in (0,1]$. At the same time, the family is subjected to Gaussian white noise. Employing a travelling wave transformation reduces the FSWBBM equations to nonlinear fractional stochastic ordinary differential equations. The R-B S-ODE approach is then used to obtain closed-form analytical solutions. This method generates various families of explicit solutions, including hyperbolic, trigonometric, and rational functions, depending on the fractional order and stochastic strength ϱ . The physical characteristics of the resulting waveforms are illustrated through two-dimensional and three-dimensional plots produced with MATLAB software. The findings confirm that the R-B S-ODE method provides a robust analytical tool for solving higher-dimensional fractional stochastic equations.

Keywords: Wazwaz-Benjamin-Bona-Mahony Equations (WBBMEs), Stochastic Partial Differential Equations, Riccati-Bernoulli Sub-ODE Method, Conformable fractional derivative, Travelling wave solutions.

(*) **Corresponding Author**:
Ahmed M. A. Adam
Department of Mathematics, College of Science, Northern Border University, Arar, Saudi Arabia

DOI: 10.12816/0062501

1. Introduction

Fractional partial differential equations (FPDEs) are utilized to model complicated phenomena across diverse areas, like viscoelastic media [1], control systems and signal processing [2], and biological systems [3], among others. Fractional derivatives, enabling the modeling of systems with non-integer order. They are widely applied in viscoelasticity, physics, and biology, and can be expressed in various forms, including the Grünwald-Letnikov, Hadamard, Riesz, Riemann-Liouville, Caputo and Conformable derivatives [4, 8].

Fractional stochastic partial differential equations (FSPDEs) are an advanced class of mathematical models that combine fractional calculus with stochastic processes to capture system exhibiting anomalous diffusion, non-integer order, and intrinsic randomness. These models generalize classical partial differential equations by incorporating derivatives of non-integer order, which enable more accurate modeling of complex behaviors found in physics, finance, and biology [9-11].

This work focuses on a family of FSWBBM equations formulated within the framework of stochastic calculus. The governing equations incorporate both conformable fractional derivative (CFD) and Gaussian white noise, driven by a standard Wiener process. The family under study includes nonlinear interactions and higher-order mixed spatial-temporal derivatives, making it analytically rich and challenging. Our objective in this study is to develop exact solutions to FSWBBM equations using R-B S-ODE technique.

Consider the following set of equations:

$$\mathfrak{D}_t^{\vartheta}\mathcal{H} + \mathfrak{D}_x^{\vartheta}\mathcal{H} + \mathcal{H}^2\mathfrak{D}_y^{\vartheta}\mathcal{H} - \mathfrak{D}_{xzt}^{3\vartheta}\mathcal{H} = \frac{\varrho}{2}(\mathcal{H} - \mathfrak{D}_{xz}^{2\vartheta}\mathcal{H})dW(t)., \quad (1.1)$$

$$\mathfrak{D}_t^{\vartheta}\mathcal{H} + \mathfrak{D}_z^{\vartheta}\mathcal{H} + \mathcal{H}^2\mathfrak{D}_x^{\vartheta}\mathcal{H} - \mathfrak{D}_{xyt}^{3\vartheta}\mathcal{H} = \frac{\varrho}{2}(\mathcal{H} - \mathfrak{D}_{xy}^{2\vartheta}\mathcal{H})dW(t), \quad (1.2)$$

$$\mathfrak{D}_t^{\vartheta}\mathcal{H} + \mathfrak{D}_y^{\vartheta}\mathcal{H} + \mathcal{H}^2\mathfrak{D}_z^{\vartheta}\mathcal{H} - \mathfrak{D}_{xxt}^{3\vartheta}\mathcal{H} = \frac{\varrho}{2}(\mathcal{H} - \mathfrak{D}_{xx}^{2\vartheta}\mathcal{H})dW(t), \quad (1.3)$$

Here $\mathcal{H}$, is a function of the spatial variables *x, y, z* and time *t*. The operators $\mathfrak{D}_x^{\vartheta}, \mathfrak{D}_y^{\vartheta}, \mathfrak{D}_z^{\vartheta}$ and $\mathfrak{D}_t^{\vartheta}$ denote the first-order CFD of order ϑ with respect to spatial variables and time, respectively. The second-order mixed derivative is defined as $\mathfrak{D}_{xz}^{2\vartheta}\mathcal{H} = \mathfrak{D}_x^{\vartheta}(\mathfrak{D}_z^{\vartheta}\mathcal{H})$, while the third-order mixed derivative is given by $\mathfrak{D}_{xyt}^{3\vartheta}\mathcal{H} = \mathfrak{D}_x^{\vartheta}(\mathfrak{D}_y^{\vartheta}(\mathfrak{D}_t^{\vartheta}\mathcal{H})$.

Here $W(t)$ is a standard Wiener process (SWP), and ϱ is noise strength. The SWP satisfies the following conditions [12]

- $W(0) = 0$.
- $W(t)$ is continuous.
- $W(t)$ has independent increments.
- $W(t) - W(\tau) \sim N(0, t-\tau)$ for $0 \le \tau \le t$, and , $N(0, t-\tau)$ represents a normal distribution.

Consequently, the expectation satisfies $E[e^{\varrho W(t)}] = e^{\left(\frac{\varrho^2}{2}t\right)}$.

In addition to these properties, it is important to emphasize that a SWP, being a Gaussian stochastic process, can be expressed as a linear combination of independent normally distributed random variables [12, 38, 39].

R-B S-ODE method is recognized as a powerful and efficient analytical method for deriving exact solutions of various NLPDEs [13]. A notable characteristic of this approach is its ability to derive an infinite set of solutions through the application of a Bäcklund transformation. The method has been applied to numerous nonlinear models arising in diverse areas such as fluid mechanics, plasma, and nonlinear optics [14-16]. In this study, the R-B S-ODE method is employed to derive analytical solutions to FSWBBM equations.

In the limiting case $\vartheta = 1$, $\varrho = 0$, Eqs. (1.1)-(1.3) reduces to the classical WBBM [17] equations.

$$\mathcal{H}_t + \mathcal{H}_x + \mathcal{H}^2\mathcal{H}_y - \mathcal{H}_{xzt} = 0. \quad (1.4)$$

$$\mathcal{H}_t + \mathcal{H}_z + \mathcal{H}^2\mathcal{H}_x - \mathcal{H}_{xyt} = 0. \quad (1.5)$$

$$\mathcal{H}_t + \mathcal{H}_y + \mathcal{H}^2\mathcal{H}_z - \mathcal{H}_{xxt} = 0. \quad (1.6)$$

Various methods have been developed to obtain solutions to Eqs. (1.4)-(1.6), these include tanh-sech method [17], modified extended tanh-function approach [18], Sardar-subequation techniques [19], the tanh-coth approach [20], several auxiliary equation-base techniques [21-23]. Other approaches involve the simple ansatz procedure [24], the modified exp-function strategy [25], the modified simple equation and R-B S-ODE methods [26], the exp ($-\phi(\psi)$)-expansion technique [27]. Additionally, expansion techniques such as the (G'/G^2)-expansion techniques [28, 29], the Sine-Gordon expansion technique [30], generalized Kudryashov method and optimal homotopy asymptotic strategy [31]. Moreover, numerical solutions based on the Sinc-collocation method have been used [32].

Furthermore, numerous research efforts have been devoted to the study of stochastic WBBM equations. For instance, [33] investigated the bifurcation solutions, while [34, 35] applied modified tanh-coth methods. In [36], $\mathcal{G}'/(\mathcal{G}' + \mathcal{G} + \mathcal{A})$-expansion and the modified $\mathcal{G}'/\mathcal{G}^2$-expansion methods are used. The authors of [37] employed the F-expansion method.

The application of the R-B S-ODE method to the FSWBBM equations has received limited attention in the existing literature. Accordingly, this study is devoted to deriving diverse novel exact solutions of the FSWBBM equations, thereby enhancing our understanding of their physical behaviors.

The article is structured as follows: Section2, introduces the CFD. Section 3 outlines the steps of the method. Section 4 presents exact solutions of the family of FSWBBM equations. Section 5 provides a discussion. Finally, Section 6 summarize the conclusion drawn from the study.

2. Foundation

This section presents the CFD and summarize its fundamental characteristics.

Definition [8]. Let $\mathcal{M}(t)$ be real-valued function defined on $[0,\infty)$. The CFD of order $\vartheta \in (0,1]$ for $\mathcal{M}$ is defined as

$$\mathfrak{D}_t^{\vartheta}\mathcal{M}(t) = \lim_{\delta \to 0} \frac{\mathcal{M}(t + \delta t^{1-\vartheta}) - \mathcal{M}(t)}{\delta}, \forall \delta > 0.$$

If this limit exists, for $\mathcal{M}$ and $\mathcal{N}$, then

$$\mathfrak{D}_t^{\vartheta} t^k = k t^{k-\vartheta}, k \in \mathbb{R},$$

$$\mathfrak{D}_t^{\vartheta} b = 0,$$

$$\mathfrak{D}_t^{\vartheta}(b\mathcal{M} + d\mathcal{N}) = b\mathfrak{D}_t^{\vartheta}\mathcal{M} + d\mathfrak{D}_t^{\vartheta}\mathcal{N},$$

$$\mathfrak{D}_t^{\vartheta}(\mathcal{M}\mathcal{N}) = \mathcal{M}\mathfrak{D}_t^{\vartheta}\mathcal{N} + \mathcal{N}\mathfrak{D}_t^{\vartheta}\mathcal{M},$$

$$\mathfrak{D}_t^{\vartheta}\left(\frac{\mathcal{M}}{\mathcal{N}}\right) = \frac{\mathcal{N}\mathfrak{D}_t^{\vartheta}\mathcal{M} - \mathcal{M}\mathfrak{D}_t^{\vartheta}\mathcal{N}}{\mathcal{N}^2},$$

$$\mathfrak{D}_t^{\vartheta}\mathcal{M}(t) = t^{1-\vartheta}\mathcal{M}',$$

$$\mathfrak{D}_t^{\vartheta}\mathcal{M}[\mathcal{N}(t)] = t^{1-\vartheta}\mathcal{N}'(t)\mathcal{M}'[\mathcal{N}(t)],$$

where b and d are constants.

The conformable fractional derivative is adopted in this work because, in contrast to the Caputo and Riemann–Liouville derivatives, it preserves many structural properties of the classical derivative, the detailed discussion and comparative remarks can be found in [8, 40, 41]. Moreover, the CFD admits a clear physical and geometrical interpretation as discussed in [42]. The motivation underling the main advantages and key limitations of CFD is discussed in detail, and the reader is referred to the relevant literature; see for example references [8, 41].

3. Description of the R-B S-ODE method [13]

Consider the following space-time FPDE:

$$G(\mathcal{M}, \mathfrak{D}_t^{\vartheta}\mathcal{M}, \mathfrak{D}_x^{\vartheta}\mathcal{M}, \mathfrak{D}_y^{\vartheta}\mathcal{M}, \mathfrak{D}_z^{\vartheta}\mathcal{M}, \mathfrak{D}_{tt}^{2\vartheta}\mathcal{M}, \mathfrak{D}_{tx}^{2\vartheta}\mathcal{M}, \dots) = 0, \quad 0 < \vartheta \le 1, \tag{3.1}$$

where G represents a polynomial in $\mathcal{M}(x, y, z, t)$ and its associated derivatives. The R-B S-ODE method is carried out through the following steps.

(1) Using the transformation $\mathcal{M}(x,y,z,t) = \mathcal{M}(\xi)$, with $\xi = (px^{\vartheta} + qy^{\vartheta} + rz^{\vartheta} - \omega t^{\vartheta})/\vartheta$, where p, q, r and ω are constants. Eq. (3.1) transformed to an ODE:

$$Q(\mathcal{M}, \mathcal{M}', \mathcal{M}'', \dots) = 0, \tag{3.2}$$

where $\mathcal{M}' = \frac{d\mathcal{M}}{d\xi}$.

(2) Assume that Eq. (3.2) has similar solution as R-B equation

$$\mathcal{M}' = \hbar M^{2-n} + k\mathcal{M} + \ell\mathcal{M}^n, \tag{3.3}$$

where the constants $\hbar, k, \ell,$ and n are to be identified. The higher derivatives of Eq. (3.3) gives

$$\left.\begin{aligned} \mathcal{M}'' &= \hbar k(3-n)\mathcal{M}^{2-n} + \hbar^2(2-n)\mathcal{M}^{3-2n} + n\ell^2\mathcal{M}^{2n-1} + k\ell(n+1)\mathcal{M}^n + (2\hbar\ell + k^2)\mathcal{M} \\ \mathcal{M}''' &= \begin{bmatrix} \hbar k(3-n)(2-n)\mathcal{M}^{1-n} + \hbar^2(2-n)(3-2n)\mathcal{M}^{2-2n} + n\ell^2(2n-1)\mathcal{M}^{2n-2} \\ + k\ell n(n+1)\mathcal{M}^{n-1} + (2\hbar\ell + k^2) \end{bmatrix}\mathcal{M}' \end{aligned}\right\}. \tag{3.4}$$

The following set are solutions of Eq. (3.3)

Set-1. For $n=1$,

$$\mathcal{M} = \mathcal{C}e^{(\hbar + k + \ell)\xi}. \tag{3.5}$$

Set-2. For $n \neq 1$ and $k = \ell = 0$,

$$\mathcal{M} = \sqrt[n-1]{\hbar(n-1)(\xi + \mathcal{C})}. \tag{3.6}$$

Set-3. For $n \neq 1$, $k \neq 0$ and $\ell = 0$,

$$\mathcal{M} = \sqrt[n-1]{\mathcal{C}e^{k(n-1)\xi} - \frac{\hbar}{k}}. \tag{3.7}$$

Set-4. For $n \neq 1$, $\hbar \neq 0$, and $k^2 - 4\hbar\ell < 0$

$$\mathcal{M} = \left(-\frac{k}{2\hbar} + \frac{\sqrt{4\hbar\ell - k^2}}{2\hbar} tan\left(\frac{(1-n)\sqrt{4\hbar\ell - k^2}}{2}(\xi + \mathcal{C})\right)\right)^{\frac{1}{1-n}}, \tag{3.8}$$

and

$$\mathcal{M} = \left(-\frac{k}{2\hbar} - \frac{\sqrt{4\hbar\ell - k^2}}{2\hbar} cot\left(\frac{(1-n)\sqrt{4\hbar\ell - k^2}}{2}(\xi + \mathcal{C})\right)\right)^{\frac{1}{1-n}}. \tag{3.9}$$

Set-5. For $n \neq 1$, $\hbar \neq 0$, and $k^2 - 4\hbar\ell > 0$

$$\mathcal{M} = \left(-\frac{k}{2\hbar} - \frac{\sqrt{k^2 - 4\hbar\ell}}{2\hbar} tanh\left(\frac{(1-n)\sqrt{k^2 - 4\hbar\ell}}{2}(\xi + \mathcal{C})\right)\right)^{\frac{1}{1-n}}, \tag{3.10}$$

and

$$\mathcal{M} = \left(-\frac{k}{2\hbar} - \frac{\sqrt{k^2 - 4\hbar\ell}}{2\hbar} coth\left(\frac{(1-n)\sqrt{k^2 - 4\hbar\ell}}{2}(\xi + \mathcal{C})\right)\right)^{\frac{1}{1-n}}. \tag{3.11}$$

Set-6. For $n \neq 1$, $\hbar \neq 0$, and $k^2 - 4\hbar\ell = 0$

$$\mathcal{M} = \sqrt[1-n]{\left(\frac{1}{\hbar(n-1)(\xi + \mathcal{C})} - \frac{k}{2\hbar}\right)}, \tag{3.12}$$

where $\mathcal{C}$ is constant.

(3) Placing Eqs. (3.3) and (3.4) into Eq. (3.2) results in an algebraic equation in term of $\mathcal{M}$, whose solution yields $\hbar$, k and ℓ, these are then substituted into Eqs. (3.5)-(3.12) to provides the travelling wave solutions for Eqs. (1.1)-(1.3).

Let $\mathcal{M}_{m-1}(\xi)$ and $\mathcal{M}_m(\xi) = \mathcal{M}_m(\mathcal{M}_{m-1}(\xi))$ and be solutions of Eq. (3.3). Then, we have the following relation

$$\frac{d\mathcal{M}_m(\xi)}{d\xi}=\frac{d\mathcal{M}_m(\xi)}{d\mathcal{M}_{m-1}(\xi)}\frac{d\mathcal{M}_{m-1}(\xi)}{d\xi}=\frac{d\mathcal{M}_m(\xi)}{d\mathcal{M}_{m-1}(\xi)}\left(\hbar\mathcal{M}_{m-1}^{2-n}+\Bbbk\mathcal{M}_{m-1}+\ell\mathcal{M}_{m-1}^{n}\right),$$

which leads to

$$\frac{d\mathcal{M}_m(\xi)}{\hbar\mathcal{M}_m^{2-n}+\Bbbk\mathcal{M}_m+\ell\mathcal{M}_m^{n}}=\frac{d\mathcal{M}_{m-1}(\xi)}{\hbar\mathcal{M}_{m-1}^{2-n}+\Bbbk\mathcal{M}_{m-1}+\ell\mathcal{M}_{m-1}^{n}}.$$

Integrating with respect to ξ and simplifying, we get

$$\mathcal{M}_m(\xi)=\left(\frac{-\ell\mathcal{A}_1+\hbar\mathcal{A}_2(\mathcal{M}_{m-1}(\xi))^{1-n}}{\Bbbk\mathcal{A}_1+\hbar\mathcal{A}_2+\hbar\mathcal{A}_1(\mathcal{M}_{m-1}(\xi))^{1-n}}\right)^{\frac{1}{1-n}}, \tag{3.13}$$

where $\mathcal{A}_1$ and $\mathcal{A}_2$ being constants.

Once the solution of Eq. (3.3) is known, the Bäcklund transformation (3.13) is used to generate an infinite sequence of new solutions. Consequently, an endless sequence of solutions to Eqs. (1.1)-(1.3) can also be constructed.

4. Application of the R-B S-ODE to FSWBBM equations

Consider the wave transform

$$\mathcal{H}(x,y,z,t)=\mathcal{M}(\xi)e^{\left(\frac{\varrho}{2}\mathcal{W}(t)-\frac{1}{4}\varrho^2 t\right)},\ \ \xi=\left(px^{\vartheta}+qy^{\vartheta}+rz^{\vartheta}-\omega t^{\vartheta}\right)/\vartheta, \tag{4.1}$$

where $\mathcal{H}$ is a real function. Utilizing the CFD, the travelling wave transformation, and properties of SWP, we obtain

$$\mathfrak{D}_t^{\vartheta}\mathcal{H}=\left(-\omega\mathcal{M}'+\frac{\varrho}{2}\mathcal{M}\,d\mathcal{W}(t)\right)e^{\left(\frac{\varrho}{2}\mathcal{W}(t)-\frac{1}{4}\varrho^2 t\right)}. \tag{4.2}$$

$$\mathfrak{D}_x^{\vartheta}\mathcal{H}=p\,\mathcal{M}'e^{\left(\frac{\varrho}{2}\mathcal{W}(t)-\frac{1}{4}\varrho^2 t\right)},\ \mathfrak{D}_y^{\vartheta}\mathcal{H}=q\mathcal{M}'e^{\left(\frac{\varrho}{2}\mathcal{W}(t)-\frac{1}{4}\varrho^2 t\right)},\ \mathfrak{D}_z^{\vartheta}\mathcal{H}=r\mathcal{M}'e^{\left(\frac{\varrho}{2}\mathcal{W}(t)-\frac{1}{4}\varrho^2 t\right)}. \tag{4.3}$$

$$\mathfrak{D}_{xx}^{2\vartheta}\mathcal{H}=p^2\mathcal{M}''e^{\left(\frac{\varrho}{2}\mathcal{W}(t)-\frac{1}{4}\varrho^2 t\right)},\mathfrak{D}_{xy}^{2\vartheta}\mathcal{H}=pq\mathcal{M}''e^{\left(\frac{\varrho}{2}\mathcal{W}(t)-\frac{1}{4}\varrho^2 t\right)},\mathfrak{D}_{xz}^{2\vartheta}\mathcal{H}=pr\mathcal{M}''e^{\left(\frac{\varrho}{2}\mathcal{W}(t)-\frac{1}{4}\varrho^2 t\right)}. \tag{4.4}$$

$$\mathfrak{D}_{xxt}^{3\vartheta}\mathcal{H}=\left(-p^2\omega\mathcal{M}'''+\frac{p^2\varrho}{2}\mathcal{M}''d\mathcal{W}(t)\right)e^{\left(\frac{\varrho}{2}\mathcal{W}(t)-\frac{1}{4}\varrho^2 t\right)},\mathfrak{D}_{xyt}^{3\vartheta}\mathcal{H}=\left(-pq\omega\mathcal{M}'''+\frac{pq\varrho}{2}\mathcal{M}''d\mathcal{W}(t)\right)e^{\left(\frac{\varrho}{2}\mathcal{W}(t)-\frac{1}{4}\varrho^2 t\right)},\mathfrak{D}_{xzt}^{3\vartheta}\mathcal{H}=\left(-pr\omega\mathcal{M}'''+\frac{pr\varrho}{2}\mathcal{M}''d\mathcal{W}(t)\right)e^{\left(\frac{\varrho}{2}\mathcal{W}(t)-\frac{1}{4}\varrho^2 t\right)}. \tag{4.5}$$

4.1 Solutions for the first FSWBBM equation

Inserting Eqs. (4.1)-(4.5) into (1.1) and simplify, we obtain

$$(p-\omega)\mathcal{M}'+q\mathcal{M}^2\mathcal{M}'e^{\left(\varrho\mathcal{W}(t)-\frac{1}{2}\varrho^2 t\right)}+pr\omega\mathcal{M}'''=0. \tag{4.6}$$

Taking expectation on both sides of Eq. (4.6) result in

$$(p-\omega)\mathcal{M}'+q\mathcal{M}^2\mathcal{M}'+pr\omega\mathcal{M}'''=0. \tag{4.7}$$

Integrating Eq. (4.7) we get

$$(p-\omega)\mathcal{M}+\frac{q}{3}\mathcal{M}^3+pr\omega\mathcal{M}''=0. \tag{4.8}$$

Substituting Eq. (3.4) into (4.8) and simplify, we get

$$(p-\omega)\mathcal{M}+\frac{q}{3}\mathcal{M}^3+pr\omega(\hbar\Bbbk(3-n)\mathcal{M}^{2-n}+\hbar^2(2-n)\mathcal{M}^{3-2n}+n\ell^2\mathcal{M}^{2n-1}+\Bbbk\ell(n+1)\mathcal{M}^n+(2\hbar\ell+\Bbbk^2)\mathcal{M})=0. \tag{4.9}$$

Set $n=0$:

$$(p-\omega)\mathcal{M}+\frac{q}{3}\mathcal{M}^3+pr\omega(3\hbar\Bbbk\mathcal{M}^2+2\hbar^2\mathcal{M}^3+\Bbbk\ell+(2\hbar\ell+\Bbbk^2)\mathcal{M})=0. \tag{4.10}$$

By Collecting the like powers of $\mathcal{M}^j$ for $j=0,1,2,3,\ldots$, and equating to zero. We obtain

Coefficient of: $pr\omega\Bbbk\ell=0.$

Coefficient of: $p-\omega+pr\omega(2\hbar\ell+\Bbbk^2)=0.$

Coefficient of: $3\hbar\Bbbk pr\omega=0.$

Coefficient of: $\frac{q}{3}+2\hbar^2 pr\omega=0.$

Solving the system yields the following values:

$$\Bbbk=0,\ \hbar=\pm\sqrt{-\frac{q}{6pr\omega}},\ \ell=\frac{\omega-p}{2\hbar pr\omega}. \tag{4.11}$$

When $\frac{\omega-p}{pr\omega}>0$, from Eq. (4.11), Eq. (3.8) and Eq. (3.9), we get

$$\mathcal{H}_{1,1}(x,y,z,t)=\pm\sqrt{\frac{3(p-\omega)}{q}}\tan\left(\sqrt{\frac{\omega-p}{2pr\omega}}\left(\frac{px^{\vartheta}+qy^{\vartheta}+rz^{\vartheta}-\omega t^{\vartheta}}{\vartheta}+\mathcal{C}\right)\right)e^{\left(\frac{\varrho}{2}\mathcal{W}(t)-\frac{1}{4}\varrho^2 t\right)},$$

and

$$\mathcal{H}_{1,2}(x,y,z,t)=\pm\sqrt{\frac{3(p-\omega)}{q}}\cot\left(\sqrt{\frac{\omega-p}{2pr\omega}}\left(\frac{px^{\vartheta}+qy^{\vartheta}+rz^{\vartheta}-\omega t^{\vartheta}}{\vartheta}+\mathcal{C}\right)\right)e^{\left(\frac{\varrho}{2}\mathcal{W}(t)-\frac{1}{4}\varrho^2 t\right)},$$

where $\mathcal{C}$ is constant.

When $\frac{\omega-p}{pr\omega}<0$, we get

$$\mathcal{H}_{1,3}(x,y,z,t)=\pm\sqrt{\frac{3(\omega-p)}{q}}\tanh\left(\sqrt{\frac{p-\omega}{2pr\omega}}\left(\frac{px^{\vartheta}+qy^{\vartheta}+rz^{\vartheta}-\omega t^{\vartheta}}{\vartheta}+\mathcal{C}\right)\right)e^{\left(\frac{\varrho}{2}\mathcal{W}(t)-\frac{1}{4}\varrho^2 t\right)},$$

and

$$\mathcal{H}_{1,4}(x,y,z,t)=\pm\sqrt{\frac{3(\omega-p)}{q}}\coth\left(\sqrt{\frac{p-\omega}{2pr\omega}}\left(\frac{px^{\vartheta}+qy^{\vartheta}+rz^{\vartheta}-\omega t^{\vartheta}}{\vartheta}+\mathcal{C}\right)\right)e^{\left(\frac{\varrho}{2}\mathcal{W}(t)-\frac{1}{4}\varrho^2 t\right)},$$

where $\mathcal{C}$ is constant.

When $n\neq 1$, $\Bbbk=\ell=0$, we obtain

$$\mathcal{H}_{1,5}(x,y,z,t)=\pm\left(\sqrt{-\frac{q}{6pr\omega}}\left(\frac{px^{\vartheta}+qy^{\vartheta}+rz^{\vartheta}-\omega t^{\vartheta}}{\vartheta}+\mathcal{C}\right)\right)^{-1}e^{\left(\frac{\varrho}{2}\mathcal{W}(t)-\frac{1}{4}\varrho^2 t\right)},$$

where $\mathcal{C}$ is constant.

Appling the transformation (3.13) to the above solutions yields the following new solutions to Eq. (1.1),

$$\mathcal{H}_{1,1}^{*}(x,y,z,t)=\left(\frac{\frac{3(\omega-p)}{q}\pm\mathcal{A}\sqrt{\frac{3(p-\omega)}{q}}\tan\left(\sqrt{\frac{\omega-p}{2pr\omega}}\left(\frac{px^{\vartheta}+qy^{\vartheta}+rz^{\vartheta}-\omega t^{\vartheta}}{\vartheta}+\mathcal{C}\right)\right)}{\mathcal{A}\pm\sqrt{\frac{3(p-\omega)}{q}}\tan\left(\sqrt{\frac{\omega-p}{2pr\omega}}\left(\frac{px^{\vartheta}+qy^{\vartheta}+rz^{\vartheta}-\omega t^{\vartheta}}{\vartheta}+\mathcal{C}\right)\right)}\right)e^{\left(\frac{\varrho}{2}\mathcal{W}(t)-\frac{1}{4}\varrho^2 t\right)},$$

$$\mathcal{H}_{1,2}^{*}(x,y,z,t)=\left(\frac{\frac{3(\omega-p)}{q}\pm\mathcal{A}\sqrt{\frac{3(p-\omega)}{q}}\cot\left(\sqrt{\frac{\omega-p}{2pr\omega}}\left(\frac{px^{\vartheta}+qy^{\vartheta}+rz^{\vartheta}-\omega t^{\vartheta}}{\vartheta}+\mathcal{C}\right)\right)}{\mathcal{A}\pm\sqrt{\frac{3(p-\omega)}{q}}\cot\left(\sqrt{\frac{\omega-p}{2pr\omega}}\left(\frac{px^{\vartheta}+qy^{\vartheta}+rz^{\vartheta}-\omega t^{\vartheta}}{\vartheta}+\mathcal{C}\right)\right)}\right)e^{\left(\frac{\varrho}{2}\mathcal{W}(t)-\frac{1}{4}\varrho^2 t\right)},$$

$$\mathcal{H}_{1,3}^{*}(x,y,z,t)=\left(\frac{\frac{3(\omega-p)}{q}\pm\mathcal{A}\sqrt{\frac{3(\omega-p)}{q}}\tanh\left(\sqrt{\frac{p-\omega}{2pr\omega}}\left(\frac{px^{\vartheta}+qy^{\vartheta}+rz^{\vartheta}-\omega t^{\vartheta}}{\vartheta}+\mathcal{C}\right)\right)}{\mathcal{A}\pm\sqrt{\frac{3(\omega-p)}{q}}\tanh\left(\sqrt{\frac{p-\omega}{2pr\omega}}\left(\frac{px^{\vartheta}+qy^{\vartheta}+rz^{\vartheta}-\omega t^{\vartheta}}{\vartheta}+\mathcal{C}\right)\right)}\right)e^{\left(\frac{\varrho}{2}W(t)-\frac{1}{4}\varrho^{2}t\right)},$$

$$\mathcal{H}_{1,4}^{*}(x,y,z,t)=\left(\frac{\frac{3(\omega-p)}{q}\pm\mathcal{A}\sqrt{\frac{3(\omega-p)}{q}}\coth\left(\sqrt{\frac{p-\omega}{2pr\omega}}\left(\frac{px^{\vartheta}+qy^{\vartheta}+rz^{\vartheta}-\omega t^{\vartheta}}{\vartheta}+\mathcal{C}\right)\right)}{\mathcal{A}\pm\sqrt{\frac{3(\omega-p)}{q}}\coth\left(\sqrt{\frac{p-\omega}{2pr\omega}}\left(\frac{px^{\vartheta}+qy^{\vartheta}+rz^{\vartheta}-\omega t^{\vartheta}}{\vartheta}+\mathcal{C}\right)\right)}\right)e^{\left(\frac{\varrho}{2}W(t)-\frac{1}{4}\varrho^{2}t\right)},$$

$$\mathcal{H}_{1,5}^{*}(x,y,z,t)=\left(\frac{\frac{3(\omega-p)}{q}\pm\mathcal{A}\left(\sqrt{-\frac{q}{6pr\omega}}\left(\frac{px^{\vartheta}+qy^{\vartheta}+rz^{\vartheta}-\omega t^{\vartheta}}{\vartheta}+\mathcal{C}\right)\right)^{-1}}{\mathcal{A}\pm\left(\sqrt{-\frac{q}{6pr\omega}}\left(\frac{px^{\vartheta}+qy^{\vartheta}+rz^{\vartheta}-\omega t^{\vartheta}}{\vartheta}+\mathcal{C}\right)\right)^{-1}}\right)e^{\left(\frac{\varrho}{2}W(t)-\frac{1}{4}\varrho^{2}t\right)},$$

where $\mathcal{A}$ and $\mathcal{C}$ are constants.

The above solutions, when combined with the transformation given in Eq. (3.13), allow generation of additional solutions and so on.

The solutions of Eq. (1.2) can be derived by applying the same methodology outlined above. Accordingly, we obtain

$$\mathcal{H}_{2,1}(x,y,z,t)=\pm\sqrt{\frac{3(r-\omega)}{p}}\cot\left(\sqrt{\frac{\omega-r}{2pq\omega}}\left(\frac{px^{\vartheta}+qy^{\vartheta}+rz^{\vartheta}-\omega t^{\vartheta}}{\vartheta}+\mathcal{C}\right)\right)e^{\left(\frac{\varrho}{2}W(t)-\frac{1}{4}\varrho^{2}t\right)},\ \frac{\omega-r}{pq\omega}>0,$$

$$\mathcal{H}_{2,2}(x,y,z,t)=\pm\sqrt{\frac{3(\omega-r)}{p}}\tanh\left(\sqrt{\frac{r-\omega}{2pq\omega}}\left(\frac{px^{\vartheta}+qy^{\vartheta}+rz^{\vartheta}-\omega t^{\vartheta}}{\vartheta}+\mathcal{C}\right)\right)e^{\left(\frac{\varrho}{2}W(t)-\frac{1}{4}\varrho^{2}t\right)},\ \frac{\omega-r}{pq\omega}<0,$$

where $\mathcal{C}$ is constant.

Similarly, the solutions of Eq. (1.3) are obtained as

$$\mathcal{H}_{3,1}(x,y,z,t)=\pm\sqrt{\frac{3(q-\omega)}{r}}\tan\left(\sqrt{\frac{\omega-q}{2p^{2}\omega}}\left(\frac{px^{\vartheta}+qy^{\vartheta}+rz^{\vartheta}-\omega t^{\vartheta}}{\vartheta}+\mathcal{C}\right)\right)e^{\left(\frac{\varrho}{2}W(t)-\frac{1}{4}\varrho^{2}t\right)},\ \frac{\omega-q}{p^{2}\omega}>0,$$

and

$$\mathcal{H}_{3,2}(x,y,z,t)=\pm\sqrt{\frac{3(\omega-q)}{r}}\coth\left(\sqrt{\frac{q-\omega}{2p^{2}\omega}}\left(\frac{px^{\vartheta}+qy^{\vartheta}+rz^{\vartheta}-\omega t^{\vartheta}}{\vartheta}+\mathcal{C}\right)\right)e^{\left(\frac{\varrho}{2}W(t)-\frac{1}{4}\varrho^{2}t\right)},\ \frac{\omega-q}{p^{2}\omega}<0,$$

where $\mathcal{C}$ is constant.

4.2 Boundedness of the obtained solutions

Boundedness of the solutions to Eq. (1.1)-(1.3) is determined by the deterministic component $\mathcal{M}(\xi)$. Hyperbolic tanh-type solutions are uniformly bounded in space and yield physically admissible localized waves. In contrast, trigonometric solutions involving tan and cot, as well as coth-type and rational solutions, exhibit singularities at finite values of ξ and therefore remain unbounded, except on restricted domains. Boundedness is interpreted structurally with respect to the travelling wave variable ξ, while stochastic forcing only modulates amplitudes and does not alter the spatial structure or eliminate existing singularities.

5. Results and Discussion

5.1 Comparisons:

In this subsection, we compare our obtained solutions with those derived using other methods. First, we consider the results reported in [18] where a modified extended tanh-function method was employed. By setting $\varrho=0$, and rewriting the nonlinear terms in Eqs. (1.1)-(1.3) as $\mathcal{D}_y^{\vartheta}\mathcal{H}^3$, $\mathcal{D}_x^{\vartheta}\mathcal{H}^3$ and $\mathcal{D}_z^{\vartheta}\mathcal{H}^3$ respectively, the trigonometric (tan, cot) and hyperbolic (tanh, coth) solutions families coincide with those presented in [18]. On the other hand, by employing the Bäcklund transformation, our method yields an infinite family of exact solutions.

Next, we compare our results with those presented in [19], where solitary wave solutions were derived using the Sardar sub-equation method. By choosing $\varrho=0$ and $\vartheta=1$, the corresponding trigonometric and hyperbolic solutions reported in [19] are recovered as special cases of our results. The remaining solutions obtained in this study are not found in the literature using previously applied techniques. This highlights the robustness and effectiveness of the R-B S-ODE method in generating novel exact solutions.

5.2 Influence of white noise (WN) and fractional derivative (FD) on the solution of FSWBBM equations:

In this subsection, the influence of WN and FD on the solutions of Eqs. (1.1)-(1.3) is analyzed. Analytical solutions have been worked out for different noise strengths ϱ and fixed fractional order ϑ. The following parameters will be fixed: $\mathcal{C}=0$, $y=0$, $z=0$, $\mathcal{A}=-1$, with $x,\ t\in[-5,5]$. The simulations and corresponding visualizations are generated using the MATLAB software.

Influence of WN: Figure 1-5 illustrate the effect of multiplicative white noise on different wave profiles. In all cases, panels (I)-(IV) presented three-dimensional surfaces corresponding to increasing noise strengths ϱ=0, 0.7, 1.2, 1.7, and while panel (V) displays the associated two-dimensional profiles at a fixed time. As the noise strength increases, the wave amplitude is progressively increased, often leading to extreme peaks or singular behavior. Significantly, this amplification leaves the underlying spatial structure of each wave remains unchanged, indicating that stochastic forcing primarily acts as an amplitude-scaling process rather than altering the inherent wave structure.

Figure 1. Exhibits the space-time evolution of $\mathcal{H}^{*}_{1,3}$. The deterministic case exhibits a localized singular structure with a sharp downward spike. Increasing noise strength amplifies the wave magnitude, resulting in a singular-kink structure dominated by extreme amplitudes.

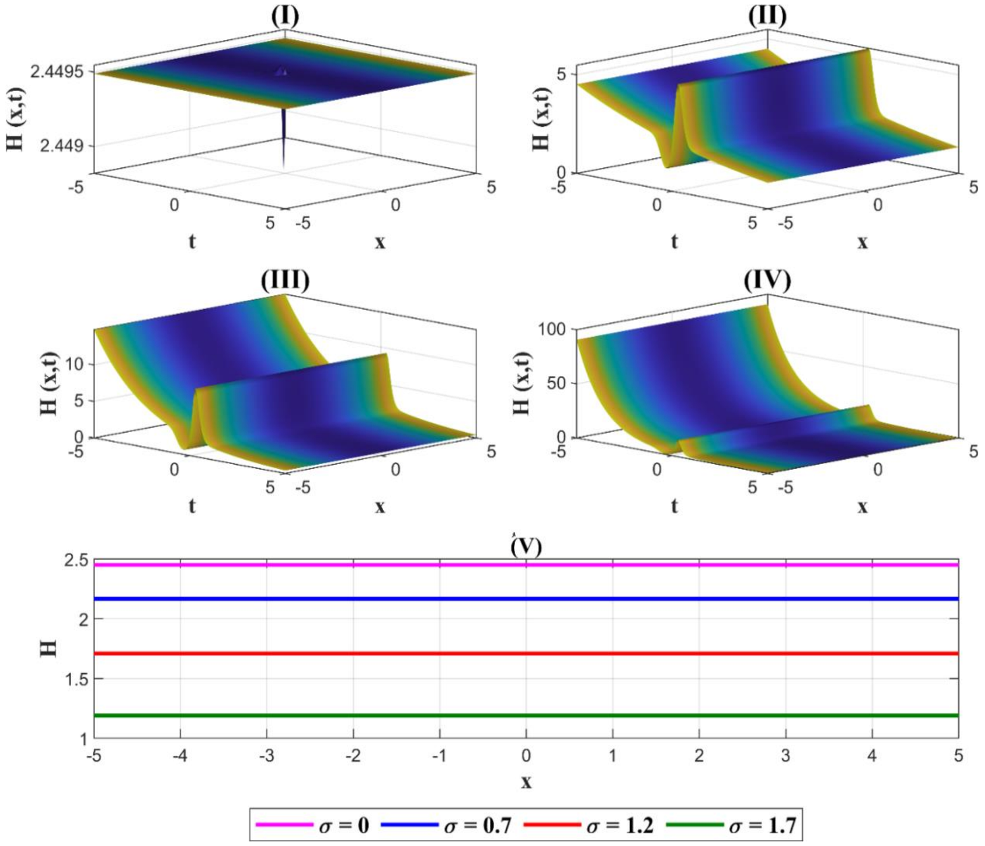

Figure 1. Panels: (I)-(IV) shows 3D-shape of $\mathcal{H}_{1,3}^{*}$ with $p = 1,\ q = 1,\ r = -\frac{1}{3}, \omega = -1,\ \vartheta = 0.25$, (I) $\varrho = 0$, (II) $\varrho = 0.7$, (III) $\varrho\ =\ 1.2$, and (IV) $\varrho\ = 1.7$ and panel (V) corresponding 2D-curves at $t\ = 2$.

Figure 2. Show the evolution of the wave profile $\mathcal{H}_{2,2}$. The solution forms a singular-kink wave whose spike height increases progressively with noise strength.

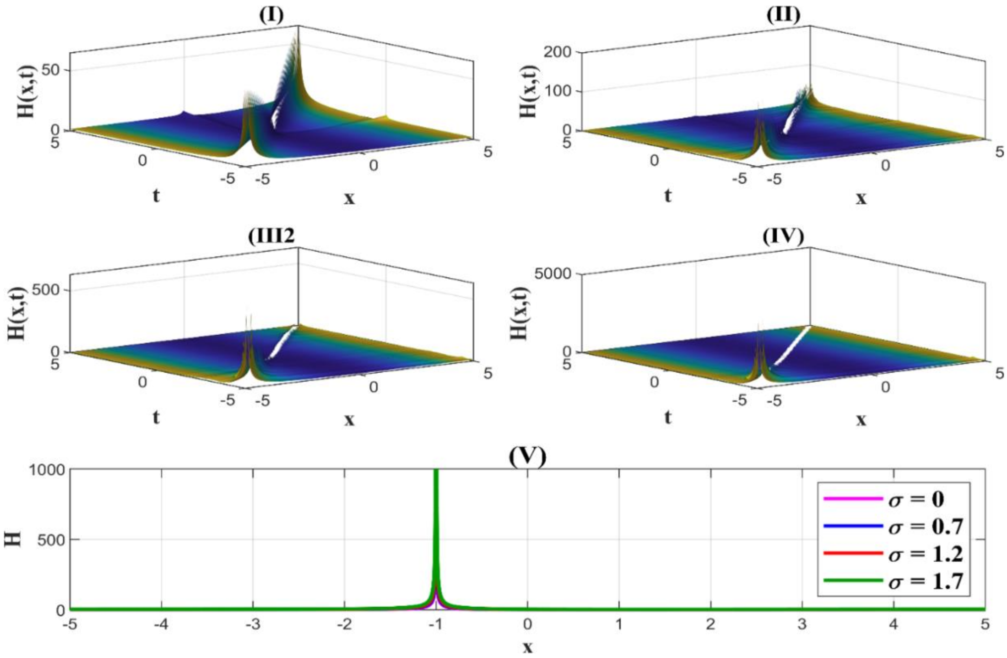

Figure 2. Panels: (I)-(IV) shows 3D-shape of $\mathcal{H}_{2,2}$ for $p = 1,\ q = 1,\ r = 0.1,\ \omega = 1,\ \vartheta = 0.5$, (I) $\varrho\ = 0$, (II) $\varrho = 0.7$, (III) $\varrho\ = 1.2$, and (IV) $\varrho\ = 1.7$ and panel (V) corresponding 2D-curves at $t\ = -1$.

Figure 3. Displays the evolution of $\mathcal{H}_{2,3}$. The deterministic solution corresponds to a stable kink connecting two distinct amplitude levels. Increasing noise preserves the kink shape while amplifying the peak amplitudes.

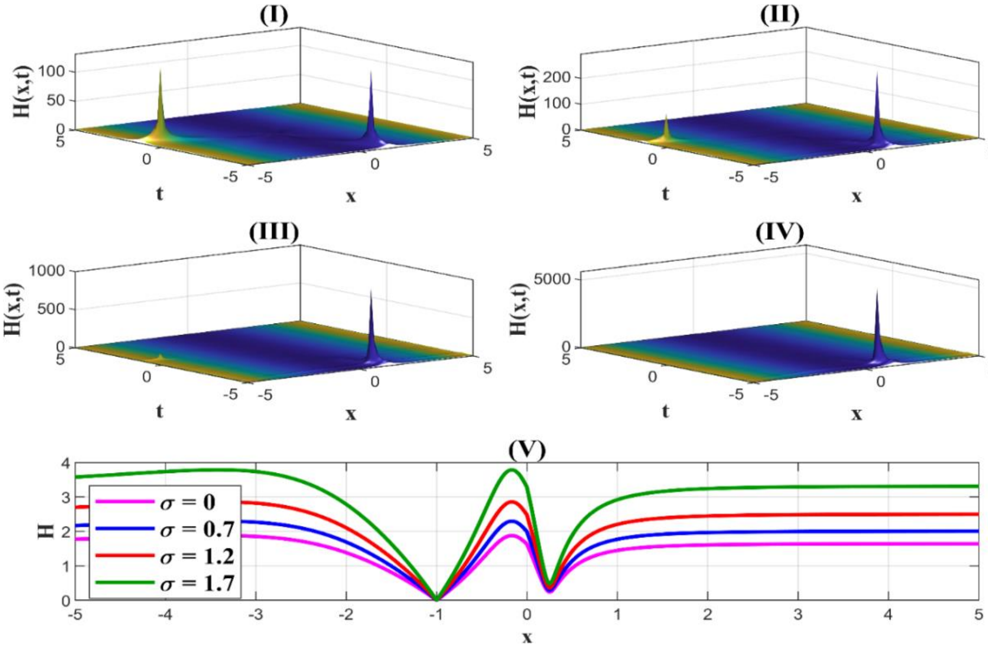

Figure 3. Panels: (I)-(IV) 3D-shape of $\mathcal{H}_{2,3}$ with $p = 1,\ q = -\frac{1}{3},\ r = 0.1,\ \omega = 1,\ \vartheta = 0.25,$ (I) $\varrho = 0$, (II) $\varrho = 0.7$, (III) $\varrho = 1.2$, and (IV) $\varrho = 1.7$ and panel (V) corresponding 2D-curves at $t = -1$.

Figure 4. Presents wave dynamics of $\mathcal{H}_{3,1}$. The solution exhibits a singular periodic structure with bright singular spikes. Noise amplification strengthens the wave magnitude without modifying the periodic singular pattern.

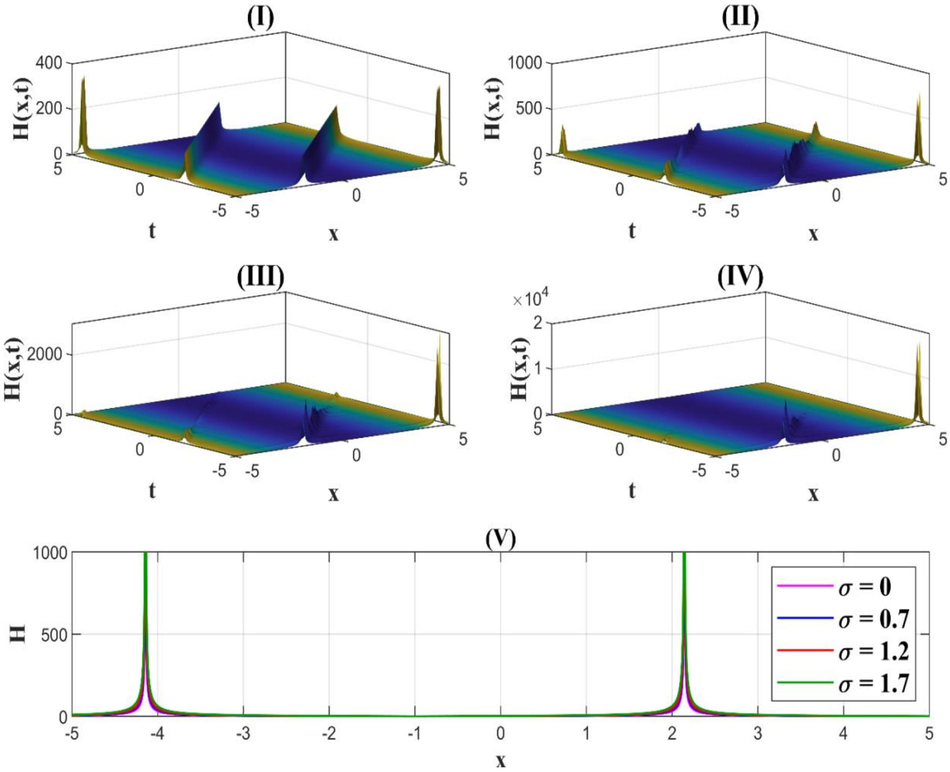

Figure 4. Panels: (I)-(IV) 3D-shape of $\mathcal{H}_{3,1}$ with $p = 1,\ q = 0.5,\ r = -0.3,\ \omega = 1,\ \vartheta = 1,$ (I) $\varrho = 0$, (II) $\varrho = 0.7$, (III) $\varrho = 1.2$, and (IV) $\varrho = 1.7$ and panel (V) corresponding 2D-curves at $t = -1$.

Figure 5. The wave surface of $\mathcal{H}_{3,4}$. The wave displays a bright singular structure that preserves its spatial structure under stochastic forcing, while exhibiting progressively stronger amplitude amplification and more pronounced peaks.

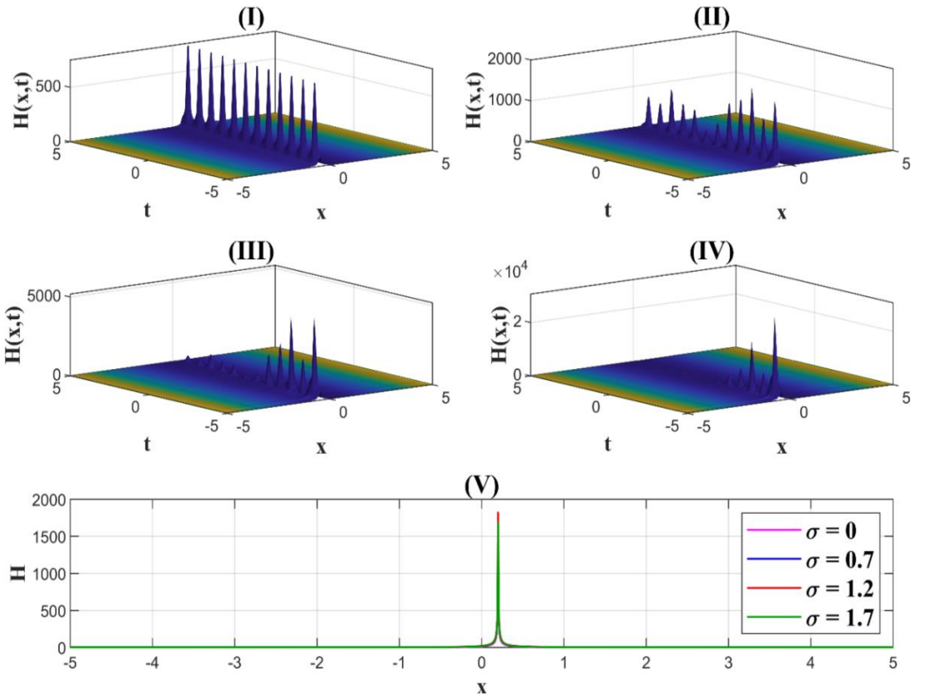

Figure 5. Panels: (I)-(IV) shows 3D-shape of $\mathcal{H}_{3,4}$ with $p = 5$, $q = 1$, $r = -0.3$, $\omega = 0.5$, $\vartheta = 1$, (I) $\varrho = 0$, (II) $\varrho = 0.7$, (III) $\varrho = 1.2$, and (IV) $\varrho = 1.7$ and panel (V) corresponding 2D-curves at $t = 2$.

Influence of CFD: Figures 6-10 demonstrate the effect of varying the conformable fractional order ϑ on the wave solutions. Panels (I)-(IV), present three-dimensional profiles corresponding to different values of order $\vartheta = 0.25, 0.5, 0.8$, and 1, while panel (V) shows the corresponding two-dimensional profiles. The results indicate that the fractional order significantly influences wave existence, shape, and stability, as well as the occurrence or absence of singular properties. In general, increasing ϑ tends to stabilize the wave profiles, leading to more regular structures and weaker singular characteristic.

Figure 6. Illustrates the wave profiles of $\mathcal{H}^{*}_{3,1}$. The lower fractional orders produce singular bright solitary-wave like structures, whereas higher values of ϑ yield smoother bright soliton-like profiles.

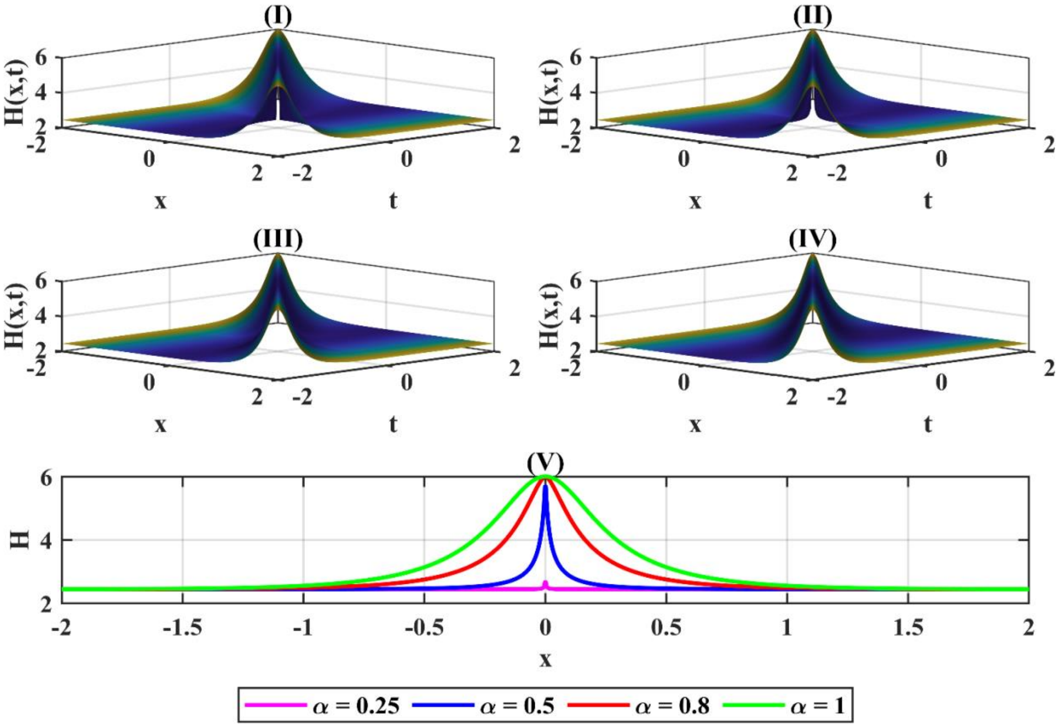

Figure 6. Panels: (I)-(IV) shows 3D-shape of $\mathcal{H}_{1,3}^{*}$ with $p = 1,\ q = 1,\ r = -\frac{1}{3},\ \omega = -1,\ \varrho = 0,$ and $A = -1$. (I) $\vartheta = 0.25$, (II) $\vartheta = 0.5$, (III) $\vartheta = 0.8$, (IV) $\vartheta = 1$ and panel (V) corresponding 2D-curves at $t = 0$.

Figure 7. Shows the evolution of singular structures under varying ϑ. The solution transitions from localized singular spike waves to singular solitary waves with kink-like skewness.

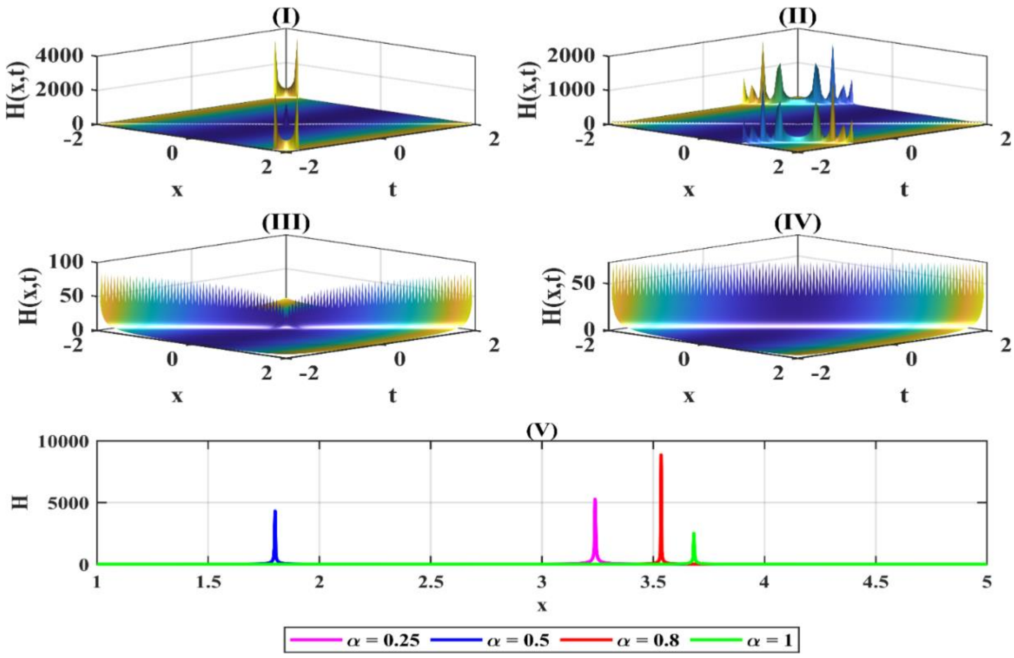

Figure 7. Panels: (I)-(IV) shows 3D-shape of $\mathcal{H}_{2,2}$ with $p = 1,\ q = 1,\ r = 0.1,\ \omega = 1,\ \varrho = 0$, (I) $\vartheta = 0.25$, (II) $\vartheta = 0.5$, (III) $\vartheta = 0.8$, (IV) $\vartheta = 1$ and panel (V) corresponding 2D-curves at $t = -1$.

Figure 8. Presents the wave dynamics of $\mathcal{H}_{2,3}$. At low ϑ, the solution exhibits a pronounced singular dark soliton, which evolves into a smooth dark soliton-like structure as ϑ increases.

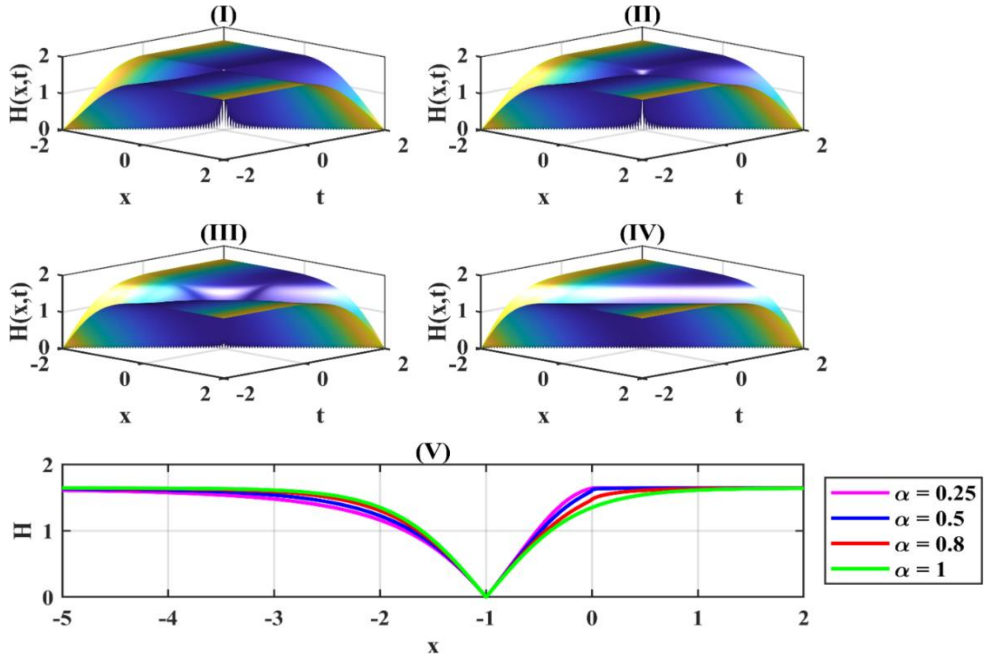

Figure 8. Panels: (I)-(IV) shows 3D-shape of $\mathcal{H}_{2,3}$ with $p = 1,\ q = -\frac{1}{3},\ r = 0.1,\ \omega = 1,\ \varrho = 0,$ (I) $\vartheta = 0.25$, (II) $\vartheta = 0.5$, (III) $\vartheta = 0.8$, (IV) $\vartheta = 1$ and panel (V) corresponding 2D-curves at $t = -1$.

Figure 9. Depicts the wave profiles of $\mathcal{H}_{3,1}$ for different fractional orders. Singular solitary-wave structures dominate at lower ϑ, while higher values lead to a singular kink-type form.

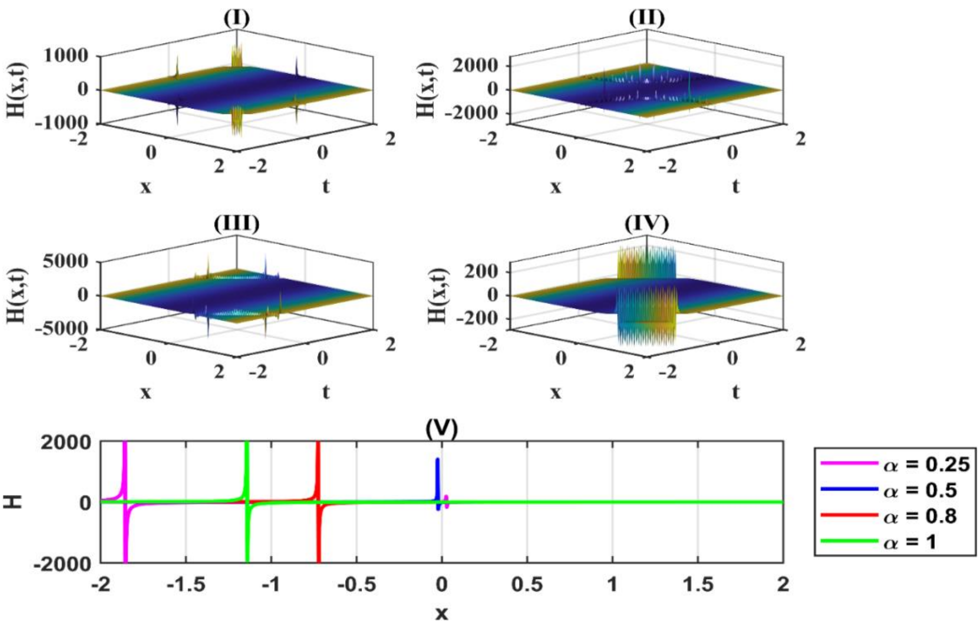

Figure 9. Panels: (I)-(IV) shows 3D-shape of $\mathcal{H}_{3,1}$ with $p = 1,\ q = 0.5,\ r = -0.3,\ \omega = 1,\ \varrho = 0,$ (I) $\vartheta = 0.25$, (II) $\vartheta = 0.5$, (III) $\vartheta = 0.8$, (IV) $\vartheta = 1$ and panel (V) corresponding 2D-curves at $t = 2$.

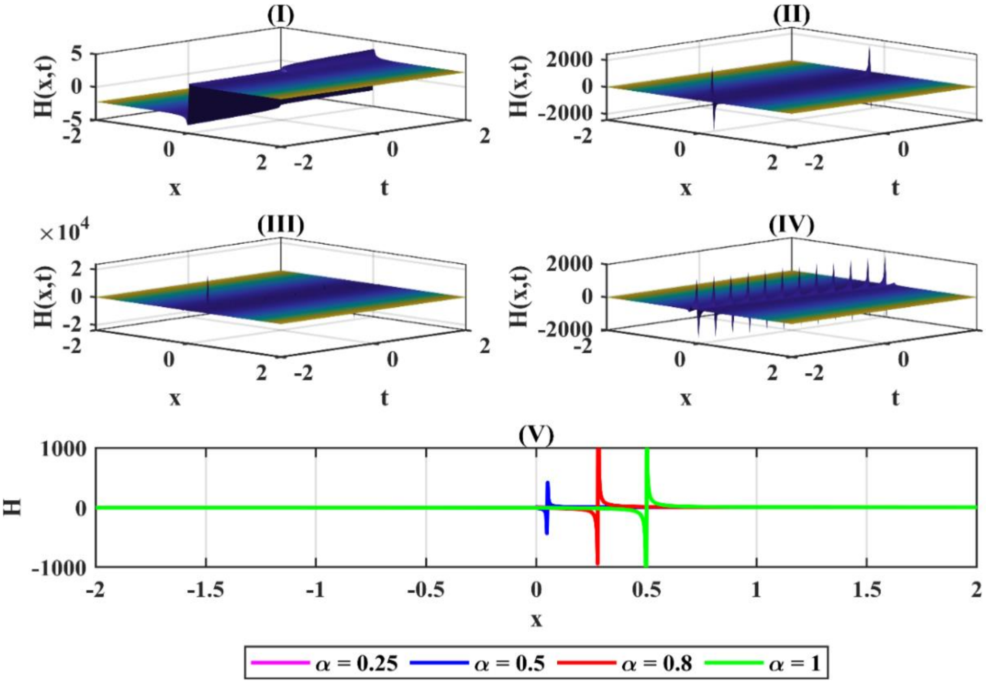

Figure 10. Panels: (I)-(IV) shows 3D-shape of $\mathcal{H}_{3,4}$ with $p = 5,\ q = 1,\ r = -0.3,\ \omega = 0.5,\ \varrho = 0,$ (I) $\vartheta = 0.25$, (II) $\vartheta = 0.5$, (III) $\vartheta = 0.8$, (IV) $\vartheta = 1$ and panel (V) corresponding 2D-curves at $t = 5$.

Figure 10. displays singular wave patterns for varying ϑ. The solution exhibits a transition from single singular kinks to strong multi-singular spike structures, with spatial locations remaining fixed and amplitudes varying progressively.

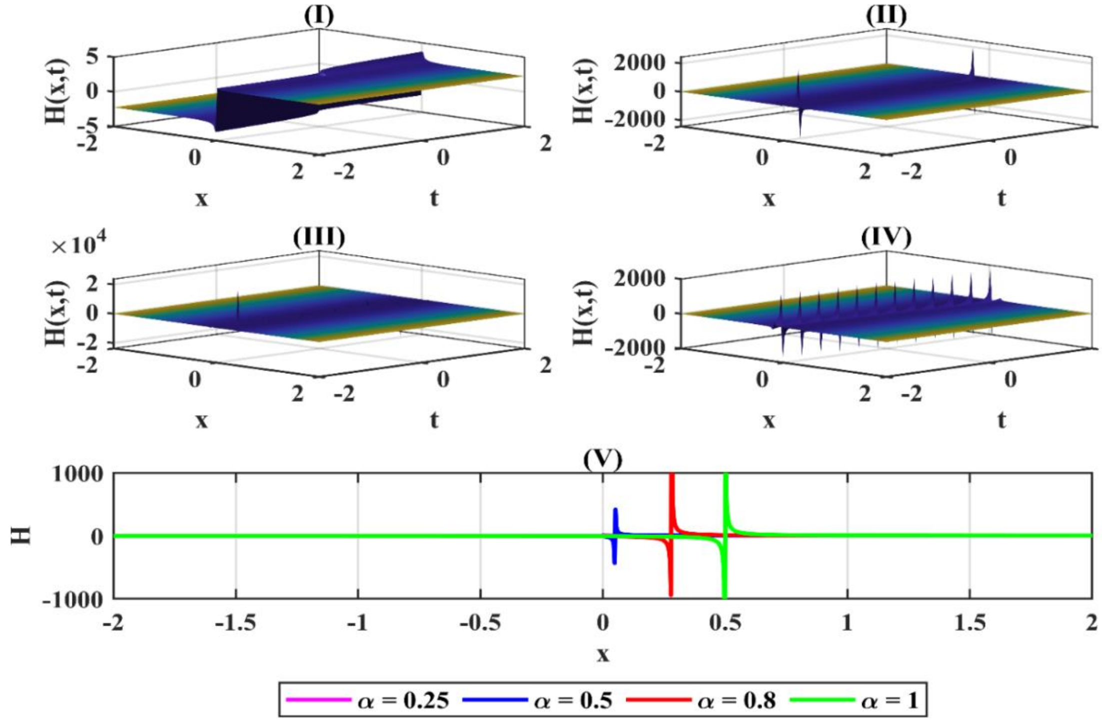

Figure 10. Panels: (I)-(IV) shows 3D-shape of $\mathcal{H}_{3,4}$ with $p = 5,\ q = 1,\ r = -0.3,\ \omega = 0.5,\ \varrho = 0,$ (I) $\vartheta = 0.25$, (II) $\vartheta = 0.5$, (III) $\vartheta = 0.8$, (IV) $\vartheta = 1$ and panel (V) corresponding 2D-curves at $t = 5$.

6. Conclusions

In this paper, the influence of WN and fractional order on the solutions of the FSWBBM equations have been investigated. A variety of travelling waves solutions for the FSWBBM equations were obtained using R-B S-ODE method. These solutions include bright, periodic bright, a combination of bright and dark singular periodic, and singular dark waves. 2D and 3D plots of these solutions are presented to illustrate the physical behavior. Based on the findings, the R-B S-ODE method possesses several advantages: it is simple, computationally efficient, and capable of yielding an infinite sequence of exact solutions. As such, it proves to be a robust scheme for resolving FSWBBM equations. Future research will extend the outcomes of this investigation to explore exact solutions of complex FSPDEs models arising in mathematics and physics.

7. References

Mainardi, F. (2022). Fractional calculus and waves in linear viscoelasticity: An introduction to mathematical models. World Scientific Publishing. https://doi.org/10.1142/p926

Monje, C. A., Chen, Y., Vinagre, B. M., Xue, D., & Feliu, V. (2010). Fractional-order systems and controls: Fundamentals and applications. Springer. https://doi.org/10.1007/978-1-84996-335-0

Magin, R. L. (2006). Fractional calculus in bioengineering. CRC Press.

Herrmann, R. (2014). Fractional calculus: An introduction for physicists (2nd ed.). World Scientific Publishing. https://doi.org/10.1142/8934

Obembe, A. D., Al-Yousef, H. Y., Hossain, M. E., & Abu-Khamsin, S. A. (2017). Fractional derivatives and their applications in reservoir engineering problems: A review. Journal of Petroleum Science and Engineering, 157, 312–327.

https://doi.org/10.1016/j.petrol.2017.07.035

Machado, J. T., Kiryakova, V., & Mainardi, F. (2011). Recent history of fractional calculus. Communications in Nonlinear Science and Numerical Simulation, 16(3), 1140–1153. https://doi.org/10.1016/j.cnsns.2010.05.027

Teodoro, G. S., Machado, J. A. T., & de Oliveira, E. C. (2019). A review of definitions of fractional derivatives and other operators. Journal of Computational Physics, 388, 195–208. https://doi.org/10.1016/j.jcp.2019.03.008

Khalil, R., Al Horani, M., Yousef, A., & Sababheh, M. (2014). A new definition of fractional derivative. Journal of Computational and Applied Mathematics, 264, 65–70. https://doi.org/10.1016/j.cam.2014.01.002

Sobczyk, K. partial differential equations and its application. Advances in Difference Equations, 2015:117 https://doi.org/10.1186/s13662-015-0452-4

Yasmin, H., Alyousef, H. A., Asad, S., Khan, I., Matoog, R. T., & El-Tantawy, S. A. (2024). The Riccati-Bernoulli sub-optimal differential equation method for analyzing the fractional Dullin-Gottwald-Holm equation and modeling nonlinear waves in fluid media. AIMS Mathematics, 9(6), 16146–16167. https://doi.org/10.3934/math.2024781

Abdelrahman, M. A. E. (2018). A note on Riccati–Bernoulli subODE method combined with complex transform method applied to fractional differential equations. Nonlinear Engineering, 7(4), 279–285. https://doi.org/10.1515/NLENG-2017-0145

Shehata, M.S.M. (2016). A New Solitary Wave Solution of the Perturbed Nonlinear Schrodinger Equation Using a Riccati Bernoulli Sub-ODE Method. International Journal of Physical Sciences, 11, 80-84. https://doi.org/10.5897/IJPS2015.4442

Wazwaz, A. (2017). Exact Soliton and Kink Solutions for New (3+1)-Dimensional Nonlinear Modified Equations of Wave Propagation. Open Engineering, 7(1), 169-174.

https://doi.org/10.1515/eng-2017-0023

Mamun, A. A., An, T., Shahen, N. H. M., Ananna, S. N., Foyjonnesa, F., Hossain, M. F., & Muazu, T. (2020). Exact and explicit travelling-wave solutions to the family of new 3D fractional WBBM equations in mathematical physics. Results in Physics, 19, 103517.

https://doi.org/10.1016/j.rinp.2020.103517

Rezazadeh, H., Inc, M., & Baleanu, D. (2020). New solitary wave solutions for variants of (3+1)-dimensional Wazwaz-Benjamin-Bona-Mahony equations. Frontiers in Physics, 8, 332.

https://doi.org/10.3389/fphy.2020.00332

Mamun, A. A., Ananna, S. N., An, T., Asaduzzaman, M., & Miah, M. M. (2022). Solitary wave structures of a family of 3D fractional WBBM equation via the tanh-coth approach. Partial Differential Equations in Applied Mathematics, 5, 100237.

https://doi.org/10.1016/j.padiff.2021.100237

Mamun, A. A., Ananna, S. N., Gharami, P. P., An, T., Liu, W., & Asaduzzaman, M. (2023). An innovative approach for developing the precise traveling wave solutions to a family of 3D fractional WBBM equations. Partial Differential Equations in Applied Mathematics, 7, 100522. https://doi.org/10.1016/j.padiff.2023.100522

Raza, N., Jhangeer, A., Rahman, R. U., Butt, A. R., & Chu, Y.-M. (2021). Sensitive visualization of the fractional Wazwaz-Benjamin-Bona-Mahony equation with fractional derivatives: A comparative analysis. Results in Physics, 25, 104171.

https://doi.org/10.1016/j.rinp.2021.104171

Akram, U., Seadawy, A. R., Rizvi, S. T. R., Younis, M., Althobaiti, S., & Sayed, S. (2021). Traveling wave solutions for the fractional Wazwaz-Benjamin-Bona-Mahony model in arising shallow water waves. Results in Physics, 20, 103725. https://doi.org/10.1016/j.rinp.2020.103725

Seadawy, A. R., Ali, K. K., & Nuruddeen, R. I. (2019). A variety of soliton solutions for the fractional Wazwaz-Benjamin-Bona-Mahony equations. Results in Physics, 12, 2234-2241.

https://doi.org/10.1016/j.rinp.2019.02.064

Shakeel, M., Attaullah, Turki N., Shah N. A., & Tag, S. M. (2023). Diversity of soliton solutions to the (3 + 1)-dimensional Wazwaz–Benjamin–Bona–Mahony equations arising in mathematical physics. Results in Physics, 51, 106624. https://doi.org/10.1016/j.rinp.2023.106624

[26] Bekir, A., Shehata, M. S. M., & Zahran, E. H. M. (2021). New perception of the exact solutions of the 3D-fractional Wazwaz-Benjamin-Bona-Mahony (3D-FWBBM) equation. Journal of Interdisciplinary Mathematics, 24(4), 867–880.

https://doi.org/10.1080/09720502.2020.1806881

Mamun, A. A., Ananna, S. N., An, T., Asaduzzaman, M., & Hasan, A. (2022). Optical soliton analysis to a family of 3D WBBM equations with conformable derivative via a dynamical approach. Partial Differential Equations in Applied Mathematics, 5, 100238.

https://doi.org/10.1016/j.padiff.2021.100238

Mamun, A. A., Shahen, N. H. M., Ananna S. N., Asaduzzaman M., & Foyjonnesa. (2021). Solitary and periodic wave solutions to the family of new 3D fractional WBBM equations in mathematical physics. Heliyon, 7, e07483. https://doi.org/10.1016/j.heliyon.2021.e07483

Shakeel, M., Manan, A., Bin Turki, N., Shah, N. A., & Tag, S. M. (2023). Novel analytical technique to find diversity of solitary wave solutions for Wazwaz-Benjamin-Bona-Mahony equations of fractional order. Results in Physics, 51, 106671.

https://doi.org/10.1016/j.rinp.2023.106671

Mamun, A. A., Ananna, S. N., An, T., Asaduzzaman, M., & Rana, M. S. (2022). Sine-Gordon expansion method to construct the solitary wave solutions of a family of 3D fractional WBBM equations. Results in Physics, 40, 105845. https://doi.org/10.1016/j.rinp.2022.105845

Gupta, A.K. & Hazarika, J. (2020). On the Solitary Wave Solutions of Modified Benjamin-Bona-Mahony Equation for Unidirectional Propagation of Long Waves. Pramana, 94, Article No. 134. https://doi.org/10.1007/s12043-020-01998-7

Barati, A. (2023). The numerical solution of the time-fractional generalized Benjamin-Bona-Mahony equation via sinc functions. International Journal of Nonlinear Analysis and Applications, 14(1), 2759-2770. https://doi.org/10.22075/ijnaa.2021.24121.2673

Elmandouh, A., & Fadhal, E. (2022). Bifurcation of exact solutions for the space-fractional stochastic modified Benjamin-Bona-Mahony equation. Fractal and Fractional, 6(12), 718.

https://doi.org/10.3390/fractalfract6120718

Agarwal, P., Hyder, A.-A., Zakarya, M., AlNemer, G., Cesarano, C., & Assante, D. (2019). Exact solutions for a class of Wick-type stochastic (3+1)-dimensional modified Benjamin-Bona-Mahony equations. Axioms, 8(4), 134. https://doi.org/10.3390/axioms8040134

Ghany, H. A., & Fathallah, A. (2014). White-noise functional solutions for Wick-type stochastic time-fractional Benjamin-Bona-Mahony equation. International Journal of Differential Equations and Applications, 13, 37–49.

Abdelkader, M., Aldwoah, K. A., Suhail, M., Kamel, A., Saber, H., Hleili, M., & Saifullah, S. (2024). Investigation of more solitary waves solutions of the stochastics Benjamin-Bona-Mahony equation under beta operator. AIMS Mathematics, 9(10), 27403-27417.

https://doi.org/10.3934/math.20241331

Al-Askar F. M., Cesarano C., & Mohammed W. W. (2023). The influence of white noise and the beta derivative on the solutions of the BBM equation. Axioms, 12 (5), 447.

https://doi.org/10.3390/axioms12050447

Øksendal, B. (2003). Stochastic Differential equations: An Introduction with Applications (6th ed.). Springer, Berlin. https://doi.org/10.1007/978-3-642-14394-6

Da Prato, G., & Zabczyk, J. (1992). Stochastic equations in Infinite Dimensions. Cambridge University Press. https://doi.org/10.1017/CBO9780511666223

Ait Brahim, A., El Ghordaf, J., El Hajaji, A., Hilal, K., & Nápoles Valdés, J. E. (2024). A comparative analysis of conformable, non-conformable, Riemann–Liouville, and Caputo fractional derivatives. European Journal of Pure and Applied Mathematics, 17(3), 1842–1854. https://doi.org/10.29020/nybg.ejpam.v17i3.5237

Abdeljawad, T. (2015). On conformable fractional calculus. Journal of Computational and Applied Mathematics, 279, 57–66. https://doi.org/10.1016/j.cam.2014.10.016

Zhao, D., & Luo, M. (2017). General conformable fractional derivative and its physical interpretation. Calcolo, 54(3), 903–917. https://doi.org/10.1007/s10092-017-0213-8